JTTEE5 13:239-247
DOI: 10.1361/10599630419409
1059-9630/$19.00 © ASM International

Analysis of Gas Flow Evolution and Shock Wave Decay in Detonation Thermal Spraying Systems

K. Ramadan and P. Barry Butler

(Submitted 29 January 2003; in revised form 14 May 2003)

The reactive Euler equations with variable gas properties are solved in both axisymmetric and plane two-dimensional flows to analyze the gas flow evolution, shock wave decay, and shock reflections in pulsed detonation thermal spraying (PDTS) systems. The gas phase governing equations are numerically solved using a high-resolution shock capturing numerical method. Expansion-compression waves are formed upon external gas expansion and persist for a long time (on the time scale of a PDTS cycle) with wide fluctuations in the gas velocity and temperature. The results show that the reflected shock wave from the substrate dies out extremely fast that micron-sized particles used in PDTS do not encounter these transients. The external shock wave decay is also analyzed for different reactive mixtures and flow geometries and is related to the truncation of the computational domain and the implementation of numerical boundary conditions at the open end boundaries.

Keywords detonation, pulsed detonation, shock decay, shock wave

1. Introduction

Detonation is an effective method of converting the chemical energy of a reactive gaseous mixture into a mechanical energy and is used in both pulsed detonation thermal spraying (PDTS) and pulsed detonation engines (PDE). In PDTS processes, the extreme gas velocities and high-energy concentration associated with the detonation phenomena are used to propel and heat a powdered material by the carrier gas prior to deposition on the target surface to form a coating layer. The PDE is a propulsion combustion device that utilizes the high-gas detonation pressures and thereby, thrusts.[1]

Figure 1 shows a schematic of a tubular barrel that can be either a thrust tube of a PDE or a tubular barrel of a PDTS device. Combustion of the gas mixture near the closed end of the tube leads to a transition from deflagration to detonation. The detonation is characterized as a high-pressure reactive shock wave that is self-supporting due to the release of chemical energy from the reactive gas mixture. The wave propagates in the hot gas stream toward the open end of the tube. Following the detonation front is an expansion wave that propagates rearward towards the breech end of the tube. Once the shock front exits the barrel, it starts decaying and the gas suddenly expands outside of the barrel.

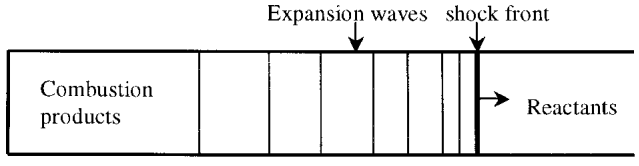

Fig. 1 Schematic illustration of a PDTS tubular barrel

K. Ramadan and **P. Barry Butler,** Department of Mechanical and Industrial Engineering, The University of Iowa, Iowa City, IA52242. e-mail: Khalid-Ramadan@uiowa.edu; Patrick-Butler@uiowa.edu.

The one-dimensional flow simulations in PDTS applications are not possible without changing the physical nature of the problem. The external gas expansion process cannot be modeled correctly with the one-dimensional flow assumption using transmissive boundary conditions. Also applying reflective boundary conditions at the substrate with the one-dimensional flow assumption means that one actually neglects the external gas expansion process that governs the gas phase evolution in the whole domain. This results in reflection of the incident shock wave with full strength just as in the shock tube problem. The multidimensional flow simulations in both PDE and PDTS applications involve dealing with large computational domains. The extension of the computational domains to the extent where the physical ambient boundary conditions can be matched results in very large domains where efficient computations are difficult. The computational domain is thus required to be truncated at some point where efficient computations are possible. The implementation of transmissive boundary conditions at the truncated boundaries is important in the analysis of both PDE and PDTS applications, where the detonation front leaves the tube very quickly and the process is mainly governed by the gas expansion process after the shock front exits the barrel. The goal of the analysis presented here is to study the gas phase evolution, shock wave decay, and shock reflections in PDTS processes. The focus here is on the gas expansion process once the shock front exits the barrel, while the analysis of detonation initiation and propagation within a PDTS tubular barrel along with verification of the transmissive boundary conditions are analyzed by

the authors and can be found in Ref 2. The transmissive boundary conditions should allow for the passage of the shock front without creating significant non-physical disturbances at the boundaries. They also are required to be applied sufficiently far away from the vicinity of the tube exit region such that the particulate phase driven by the carrier gas is not influenced by this boundary treatment. It was shown that using this treatment was successful in terms of allowing for the passage of the shock wave through the truncated boundaries.[2] It was also shown through a sort of sensitivity analysis that truncating the computational domain should also be done at some point where no effect of this boundary treatment on the particulate phase is encountered. This study aims at investigating the gas expansion process outside of a tubular barrel of a PDTS applicator, the shock wave decay and reflection phenomena that can help in a better understanding as to where to truncate the computational domain as related to shock wave decay and external gas expansion process.

Nomenclature

a	speed of sound, m/s
C_p	specific heat at constant pressure, J/kg K
C_v	specific heat at constant volume, J/kg K
d	tube diameter, m
D	detonation wave speed, m/s
e	specific internal energy, J/kg
E	total energy per unit volume, J/m^3
h	specific enthalpy, J/kg
L	tube length, m
M	Mach number
MW_i	molecular weight of species i
P	pressure, bar
r	tube radius, m
R_u	universal gas constant, J/kmol K
R	gas constant = R_u/MW
t	time, ms
T	temperature, K
T_r	typical time associated with the chemical reaction, s
u	velocity component in the axial direction, m/s
v	velocity component in the radial direction, m/s
Y_i	mass fraction of species i
Q	heat of reaction, J/kg
x	axial direction
y	radial direction

Greek Symbols

β	reaction progress variable
γ	specific heat ratio
Γ	ratio of specific enthalpy to specific internal energy
ω	chemical reaction rate, kg/m^3 s
ρ	density, kg/m^3

Subscripts

mix	mixture
o	initial state
Prod	products
react	reactants

2. Governing Equations

The governing equations of the gas-phase are the reactive Euler equations:

$$\frac{\partial \rho}{\partial t} + \frac{\partial(\rho u)}{\partial x} + \frac{\partial(\rho v)}{\partial y} = -\alpha \frac{\rho v}{y} \quad \text{(Eq 1)}$$

$$\frac{\partial(\rho u)}{\partial t} + \frac{\partial(\rho u^2 + P)}{\partial x} + \frac{\partial(\rho uv)}{\partial y} = -\alpha \frac{\rho uv}{y} \quad \text{(Eq 2)}$$

$$\frac{\partial(\rho v)}{\partial t} + \frac{\partial(\rho uv)}{\partial x} + \frac{\partial(\rho v^2 + P)}{\partial y} = -\alpha \frac{\rho v^2}{y} \quad \text{(Eq 3)}$$

$$\frac{\partial E}{\partial t} + \frac{\partial[u(E+P)]}{\partial x} + \frac{\partial[v(E+P)]}{\partial y} = -\alpha \frac{v(E+P)}{y} \quad \text{(Eq 4)}$$

$$\frac{\partial(\rho\beta)}{\partial t} + \frac{\partial(\rho u\beta)}{\partial x} + \frac{\partial(\rho v\beta)}{\partial y} = -\alpha \frac{\rho v\beta}{y} + \omega_\beta \quad \text{(Eq 5)}$$

In the above equation, x and y are respectively, the axial and radial coordinates in an axisymmetric coordinate system, or the usual Cartesian coordinates in a plane two dimensional flow, and α is an index such that:

$$\alpha = \begin{cases} 0, \text{ plane two dimensional flow} \\ 1, \text{ axisymmetric two dimensional flow} \end{cases} \quad \text{(Eq 6)}$$

where u and v are the velocity components in x and y directions, t is the time, ρ is the density, P is the pressure, β is a reaction progress variable that takes a value between 0 and 1 such that $\beta = 0$ indicates reactants, $\beta = 1$ indicates products, and $0 < \beta < 1$ indicates the reaction zone. E is the total energy given by

$$E = \rho e + \frac{1}{2}\rho(u^2 + v^2) - \rho\beta Q \quad \text{(Eq 7)}$$

where e is the specific internal energy, and Q is the energy release due to the chemical reaction. By definition, the specific internal energy is related to the specific enthalpy by

$$h = e + P/\rho \quad \text{(Eq 8)}$$

The ω_β in Eq 5 is the chemical reaction rate given by [2,3]

$$\omega_\beta = \frac{P - P_o|}{P} \frac{\rho}{T_r} (1-\beta)^{2/3} \quad \text{(Eq 9)}$$

where P is the gas pressure and P_o is the initial pressure of the uncompressed gas. The parameter T_r is a constant and represents a typical time associated with the chemical reaction. The first term in Eq 9 (i.e, $|P - P_o|/P$) serves to switch off the chemical reaction in the reactants at the initial pressure, and thus avoid using a pressure criterion to turn the reaction on and off.

The gas is assumed to be thermally perfect and the equation of state is thus:

$$P = \rho RT = \rho[C_p(T) - C_v(T)]T = \rho(\gamma(T) - 1)C_v T \quad \text{(Eq 10)}$$

where C_p and C_v are the gas specific heats at constant pressure and constant temperature, respectively, and γ(T) is the specific heat ratio:

$$\gamma(T) = \frac{C_p(T)}{C_v(T)}. \quad \text{(Eq 11)}$$

Next, the ratio of specific enthalpy to specific internal energy is defined as

$$\Gamma = \Gamma(T) = \frac{h}{e} = \frac{\int_0^T C_p(\zeta)d\zeta}{\int_0^T C_v(\zeta)d\zeta} \quad \text{(Eq 12)}$$

where ξ is a dummy integration variable. Using Eq 12 in Eq. 8 and solving for the pressure gives

$$P = (\Gamma - 1)\rho e \quad \text{(Eq 13)}$$

and the speed of sound is given by

$$a^2 = \frac{\gamma(T)P}{\rho} = \gamma(T)RT \quad \text{(Eq 14)}$$

The gas phase thermal properties are calculated based on the assumption of local chemical equilibrium. The mole fractions of the combustion products for a given reactive mixture are calculated from a chemical equilibrium code.[4] This is a Fortran code capable of performing equilibrium calculations utilizing the Gibbs free energy minimization technique. The JANAF tables[5] are then used to curve-fit the specific heats of each constituent of the mixture in a sixth-order polynomial of the form:

$$C_{pi} = a_{oi} + a_{1i}T + a_{2i}T^2 + a_{3i}T^3 + a_{4i}T^4 + a_{5i}T^5 + a_{6i}T^6 \quad \text{(Eq 15)}$$

$$C_{vi} = C_{pi} - R_u/MW_i \quad \text{(Eq 16)}$$

for a temperature range from 298.15 to 4500 K. The mixture specific heats are then calculated using the following formulas:

$$C_p = \sum_i Y_i C_{pi}, \quad C_v = C_p - R_u/MW_{mix}, \quad MW_{mix} = \frac{1}{\sum_i Y_i/MW_i} \quad \text{(Eq 17)}$$

The polynomial constants for the gas mixture are found by substituting Eq 15 into Eq 17:

$$a_j = \sum_i a_{ji}Y_i, j = 0,1,2, \ldots, 6 \quad \text{(Eq 18)}$$

The above relations apply directly to the reactants as well as the products. However, in the reaction zone both the reactants and products coexist. In this case, the specific heats are weighted by the mass fractions of the reactants and the products through the reaction progress variable:

$$C_p = \beta C_{p,Prod} + (1 - \beta)C_{p,React}, C_v = \beta C_{v,Prod} + (1 - \beta)C_{v,React} \quad \text{(Eq 19)}$$

A brief description of the numerical techniques used to solve the gas phase governing equations is presented in a companion article,[6] while the complete detail is available in Ref 3, and is thus not presented in this article.

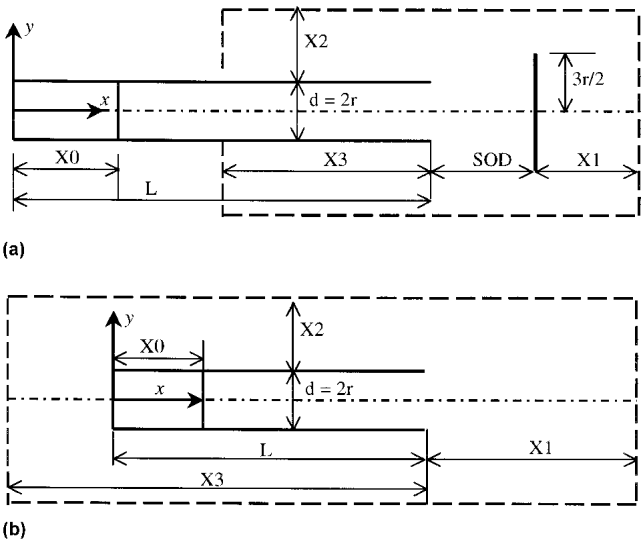

Fig. 2 Schematic illustration of the computational domain: **(a)** with a plate of diameter = 1.5*d* placed at a stand-off distance (SOD) in front of the barrel exit plane, **(b)** without a plate in front of the barrel exit

3. Results and Discussion

The gas expansion process outside the barrel and the shock reflection from the substrate are examined for axisymmetric flow using the computational domain shown in Fig. 2(a), where the dimensions are taken as $L = 0.5$ m, $d = 0.025$ m, X1 = X2 = X3 = 8*d*, SOD = 4*d*, length of the substrate = 1.5*d*. For the shock wave decay problem, both plane two-dimensional and axisymmetric flow geometries are considered, and the computational domain shown in Fig. 2(b) is used. The domain is truncated such that X1 = X2 = X3 = 15*d*, and computations are terminated before any flow crosses the boundaries, where the results are thus ensured not to be influenced by the boundary treatment at the truncated boundaries.

The chemical reaction is assumed to take place only internally (i.e., inside the barrel of the PDTS applicator), where the barrel is assumed to be filled with a reactive gas mixture. This is numerically achieved by activating the chemical reaction source term in Eq 5 only inside the tube and switching it off at the instant the detonation front reaches the tube exit plane. Detonation is initiated at the closed end of the tube by taking a small section of length X0 where the reactive gas is assumed to exist at elevated pressure and temperature. The detail of detonation initiation as well as the development of the detonation wave inside the tubular barrel can be found in Ref 2 and 3 and are not presented here. This article focuses on the gas expansion process outside the barrel and the shock wave decay during the external gas expansion process.

Figures 3-6 show snapshots of the gas pressure distribution in the whole domain at four different instants in time, while the corresponding pressure distributions along the tube centerline are shown in Fig. 7 and 8. These snapshots are chosen to show

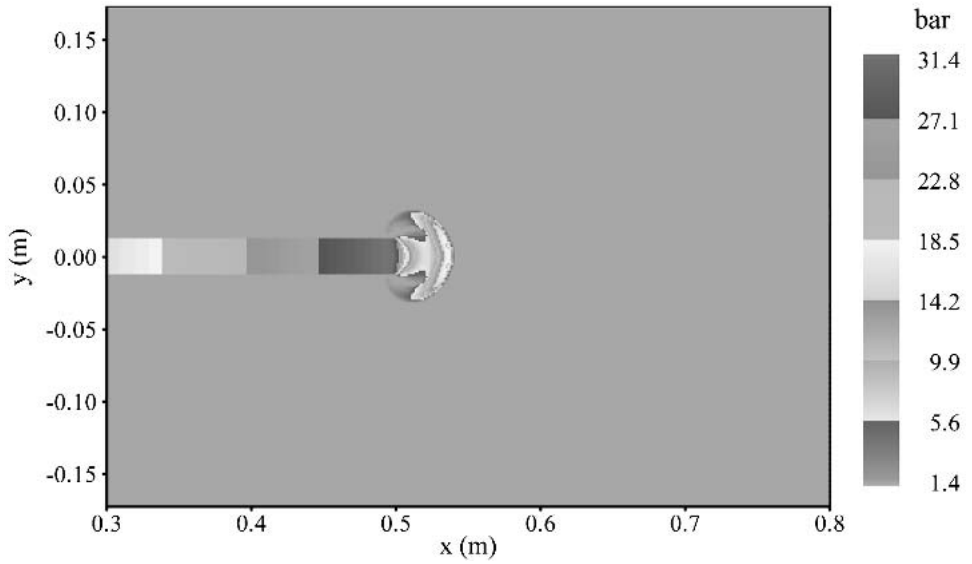

Fig. 3 Pressure distribution at the instant (time = 0.220 ms) the shock front leaves the barrel (L = 0.5 m, SOD = 4*d*)

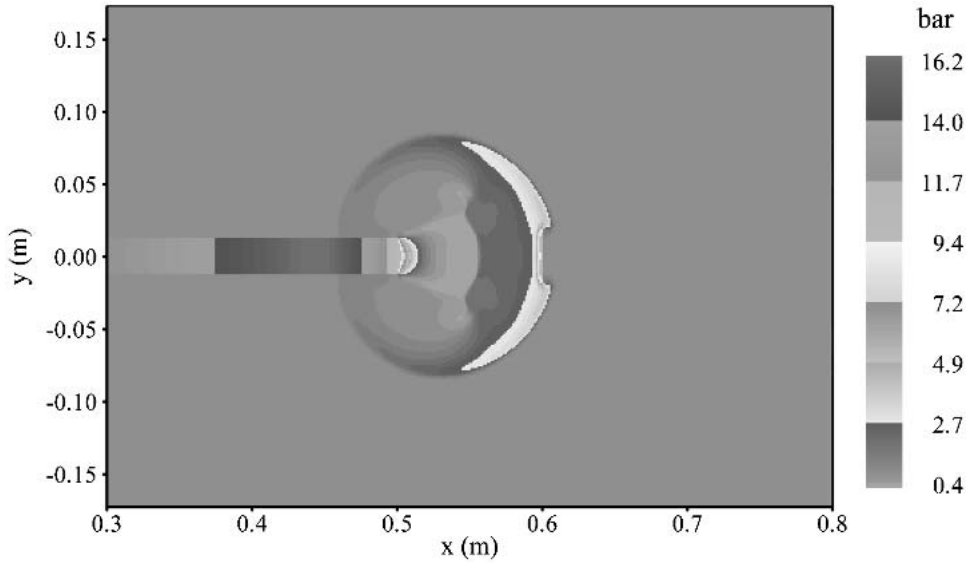

Fig. 4 Pressure distribution at the instant (time = 0.297 ms) the shock front leaves the strikes the workpiece (L = 0.5 m, SOD = 4*d*)

some important events during the gas expansion process outside the barrel of a PDTS applicator. These events include the shock wave deformation into a bow shock front upon exit from the tube as well as shock wave propagation and decay, shock reflection from the target surface, and the formation of the expansion-compression zone outside the barrel.

As soon as the shock wave exits the tube, the gas suddenly expands outside and the shock front deforms into a bow shock as shown in Fig. 3. The distribution of the gas pressure at the instant the shock wave just reaches the target plate and starts to reflect backward is shown in Fig. 4. The shape of the shock front qualitatively looks like a spherical or cylindrical shock wave that results from the explosion of a spherical or cylindrical charge.[7] It is however, quantitatively different since the shock strength varies sharply along the shock circumference with a maximum strength at the tube centerline and almost vanishing strength upstream of the tube exit plane.

Figure 4 is a snapshot of the gas pressure at the instant the shock wave has already reflected from the substrate and started propagating backward. Since the shock deforms into a bow shock, the shock front does not reach the whole plate at the same time. The first portion of the shock front at the centerline reaches the plate first. This seems to have a considerable effect on the propagation and decay of the reflected shock wave, where the reflected bow shock travels only a short distance and quickly decays and dies out. The time from the start of the shock reflection till it dies out by the incoming flow and completely disappears is about 0.06 ms (Fig. 7). In PDTS process, the upper

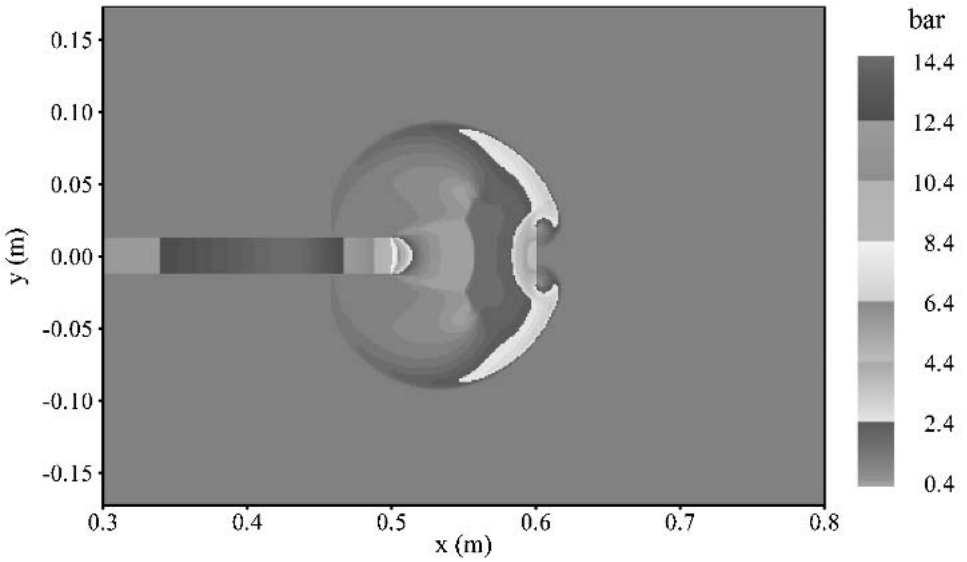

Fig. 5 Pressure distribution at the instant (time = 0.315 ms) the shock front reflects from the workpiece and propagates backwards (L = 0.5 m, SOD = 4d)

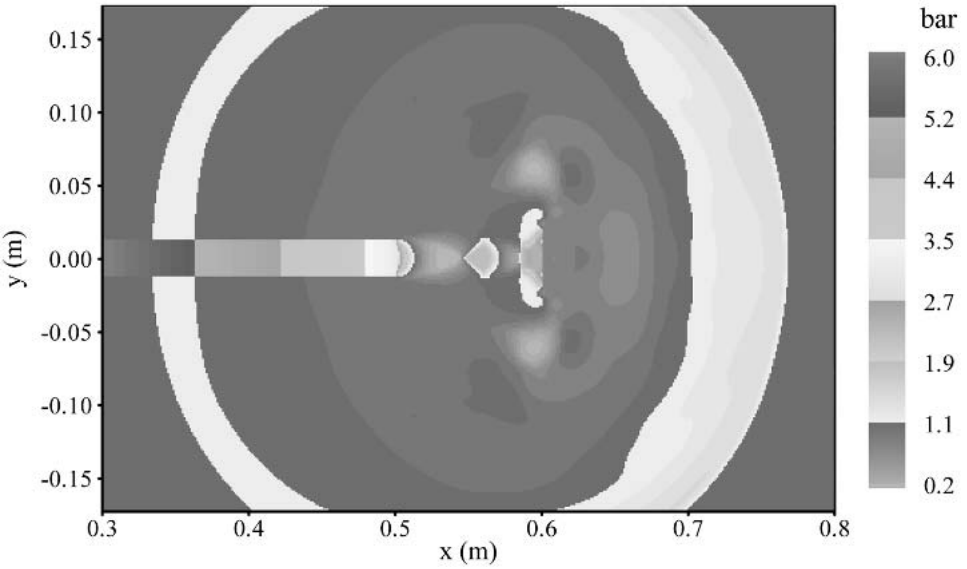

Fig. 6 Pressure distribution at time = 0.641 ms where the expansion-compression region is formed (L = 0.5 m, SOD = 4*d*)

bound of the particle velocity that can be attained is equal to the local gas velocity, which is still much less than the detonation wave speed. It can be thus concluded that in a PDTS process particles are not influenced by the shock reflection phenomena unless probably when particles are infinitely small and loaded very close to the tube exit plane.

Figure 6 is taken at a later stage where the gas experiences a series of transient interacting expansion and compression waves in the region between the tube exit plane and the plate. This phenomenon occurs since the flow becomes choked at the tube exit and thus expands supersonically outside the tube, where the expansion waves reflect from the free boundary as compression waves coalescing to form shock waves that in turn reflect from free boundaries as expansion waves. As is clear from Fig. 8, these waves persist for a long time (on the time scale of a PDTS cycle). The strength of these expansion-compression waves gradually decreases as the tube pressure decreases, and eventually disappear after the exit Mach number drops below 1.0, where the gas flow becomes subsonic at the tube exit (Fig. 9).

It may be noticed from these plots that during the sudden external gas expansion the pressure drops to about 0.1 bar creating a near vacuum at the barrel exit. Computations also show that the gas density also drops to about 0.025 kg/m^3. These values are somewhat low, and the continuum postulate of the gas phase may be questioned. The criterion used to check the valid-

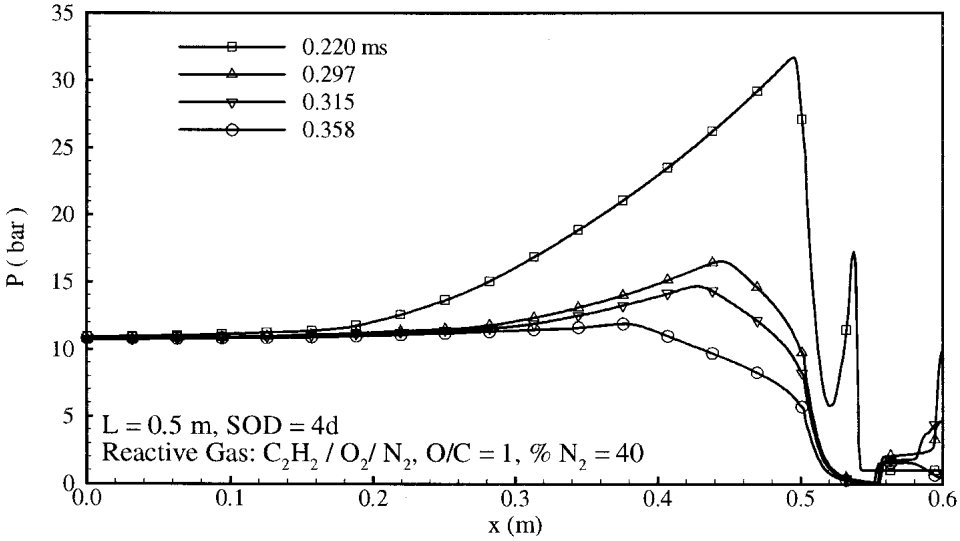

Fig. 7 Pressure distribution along the centerline at different times after the shock wave leaves barrel

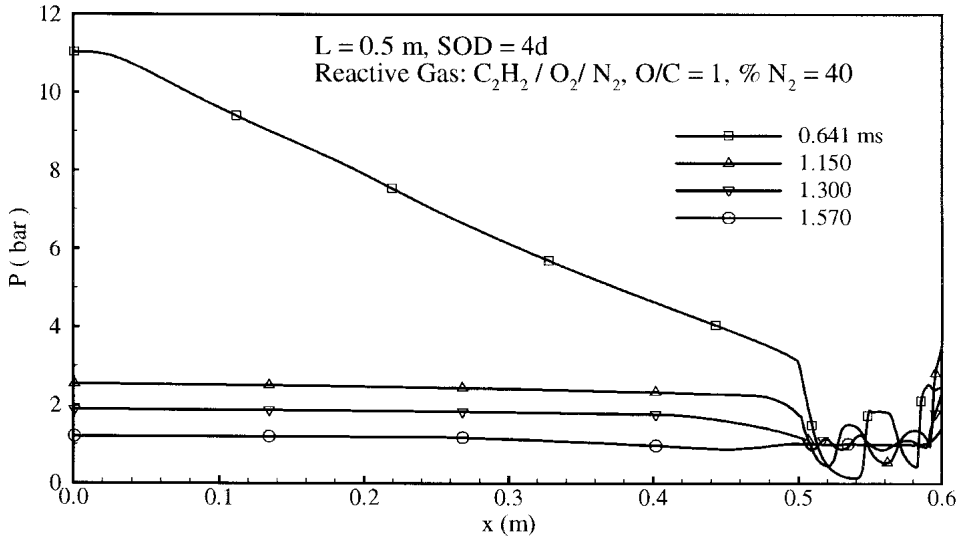

Fig. 8 Pressure distribution along the centerline at different times during the formation/decay of the expansion-compression region outside the barrel

ity of the continuum assumption in this case is the Knudsen number defined as[8]

$$Kn = \frac{1}{L} \cong \begin{Bmatrix} M/Re, & Re \cong 1 \\ M/\sqrt{Re}, & Re >> 1 \end{Bmatrix} \quad \text{(Eq 20)}$$

where α is the mean free path, L is a characteristic length of the flow field, M is the Mach number, and Re is the gas flow Reynolds number based on the barrel diameter. For the continuum postulate to be valid, the Knudsen number Kn must be less than 0.01. It was always found through all the computations performed in this work that the value of Kn in the near vacuum region is at least five times lower than this critical value and thus the continuum assumption does not fail.

Next, the external shock wave decay is examined. Several computations were performed to examine the shock wave decay for different geometrical parameters and reactive mixture compositions in both plane two-dimensional and axisymmetric flow geometries. Figure 10 shows the shock wave pressure versus shock location along the tube centerline for different tube diameters. For the tube diameters considered, the shock decay seems to have little dependency on the non-dimensional distance x_e/d measured from the exit plane along the tube centerline. For all the tube diameters considered the shock wave pressure decays to about 50% of its original strength after traveling only a distance of one tube diameter. This means that the larger the tube diameter the longer the distance the shock will travel before it decays to a certain value.

Shock wave decay in different reactive mixtures that give rise to different shock strengths is presented in Fig. 11. This shows

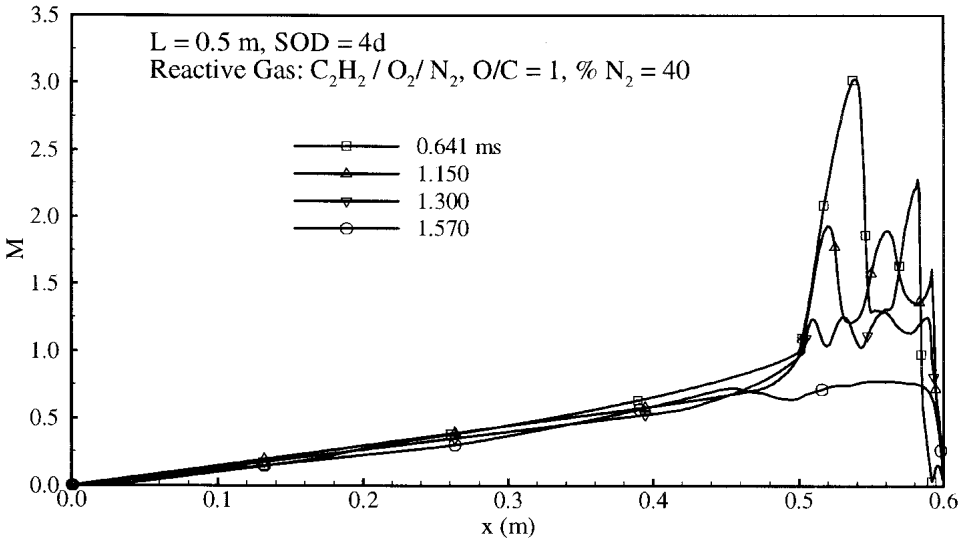

Fig. 9 Mach number distribution along the centerline at different times during the formation/decay of the expansion-compression region outside the barrel

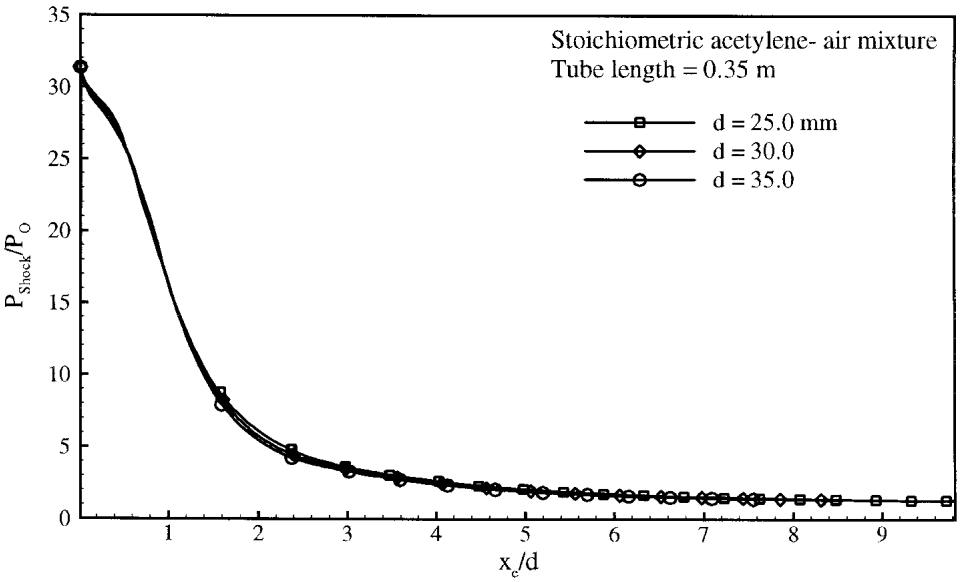

Fig. 10 Shock wave pressure versus distance for different tube diameters (x_e measured from exit plane along tube centerline)

that regardless of the initial shock strength, the decay is still very fast, and after about six tube diameters all shocks considered decay to almost the same value regardless of the initial shock strength. The decay in the shock wave is mainly due to the interaction between the high-pressure gases exiting the tube and the surroundings at ambient conditions, where the shocked gas experiences a progressive dissipation of energy. Another reason for the shock decay is due to geometrical divergence, where the geometric source terms (Eq 1-5) have a considerable effect on the shock wave decay. In plane two-dimensional flows, the shock wave decays in two directions, while in axisymmetric flow geometries, the shock wave decays essentially in three dimensions.

To see the effect of geometry on shock wave decay, computations of the shock decay for both plane two-dimensional and axisymmetric flows are performed, and the results are shown in Fig. 12 and 13. The plane two-dimensional case is simply a flow between two infinitely wide parallel plates. The effect of the geometric source terms on the shock wave decay is clearly considerable. Also clear is that in axisymmetric flow the shock decays faster in time than in the two-dimensional case (Fig. 13). For example, a shock of initial strength $P_{shock}/P_o = 35$ decays to $P_{shock}/P_o = 5$ in about 0.22 ms in axisymmetric flow and in 0.30 ms in two-dimensional flow, where the time in this plot (Fig. 13) is measured from $t = 0$ at the detonation initiation close to the breech end of the barrel.

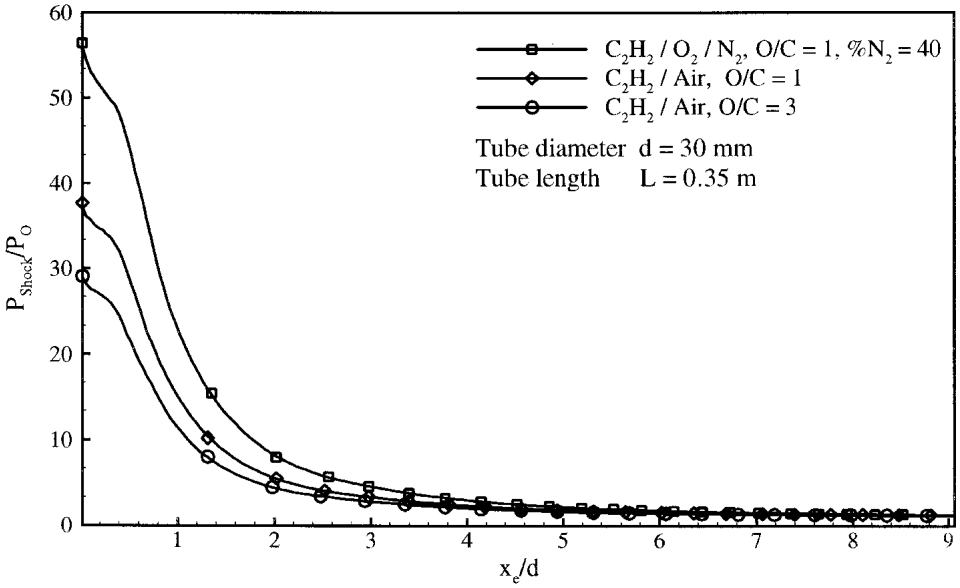

Fig. 11 Shock wave pressure versus distance for different acetyline-oxidizer mixtures (x_e measured from exit plane along tube centerline)

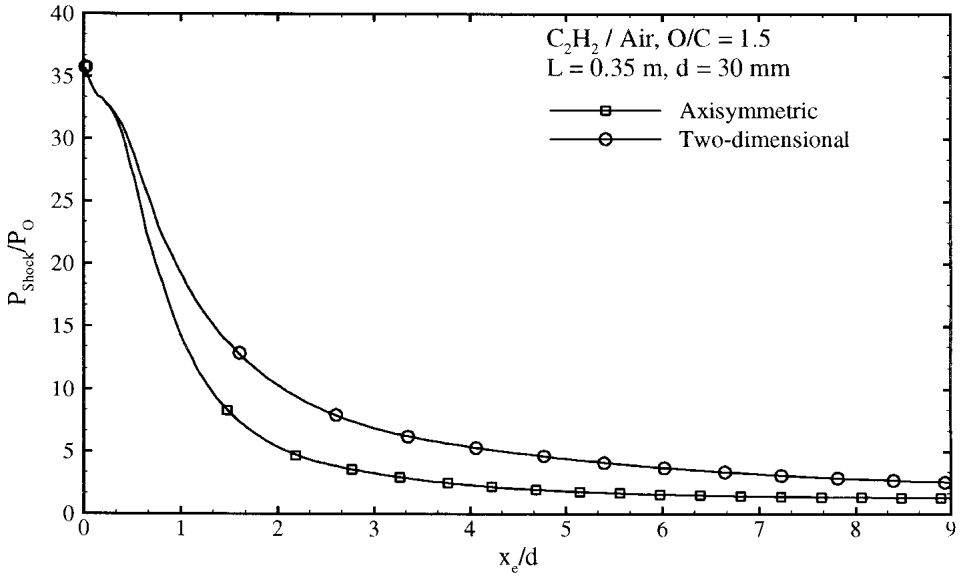

Fig. 12 Shock wave pressure versus distance for axisymmetric and two-dimensional flows (x_e measured from exit plane along tube centerline)

In both plane two-dimensional and axisymmetric flows, most of the shock decay occurs within a distance of 2-3 tube diameters, and the shock strength continues to vanish asymptotically, where it takes a long distance to vanish completely. In previous studies by the authors [2,3] it was shown that in pulsed detonation thermal spraying applications, transmissive boundary conditions should allow for the passage of the shock front through the boundaries without creating significant disturbances. It was also shown that such domain truncation should also be made at some point where the particulate phase is not influenced by the size of the domain. It was shown that truncating the domain where X1 = X2 = X3 ≥ 8*d* (Fig. 2a) was satisfactory enough that the particulate phase is not influenced by the boundary conditions. This can be related to the shock wave decay shown in Fig. 11-13. Regardless of the initial shock strength or the tube diameter, it is clear from these results that for X1 = X2 = X3 ≥ 6*d,* the shock front decayed sufficiently that further extension of the domain would only place transmissive boundaries at locations where there is almost no further shock decay.

4. Conclusions

The reactive Euler equations with variable gas properties are solved in both axisymmetric and plane two-dimensional flows to analyze the gas phase evolution, shock wave decay, and shock

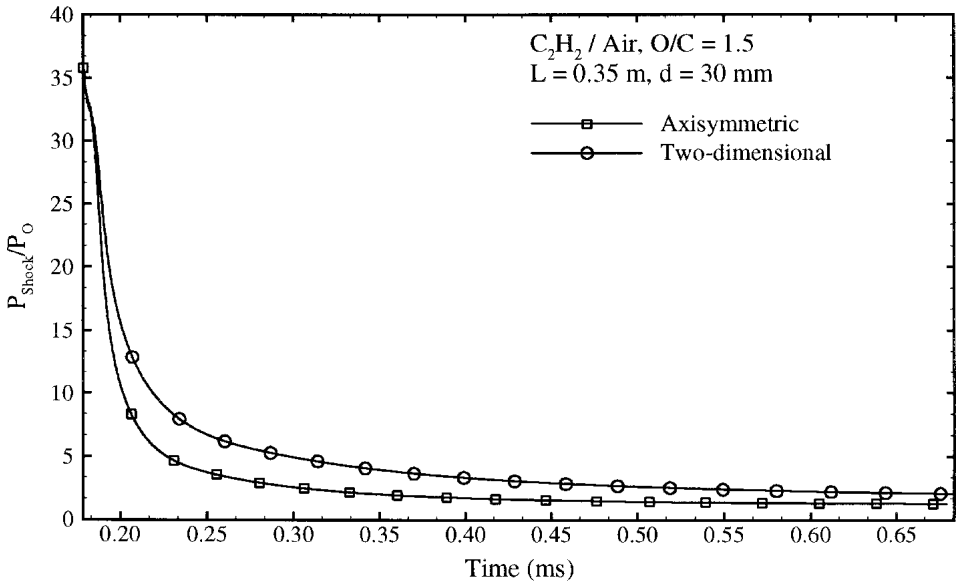

Fig. 13 Shock wave pressure versus time for axisymmetric and two-dimensional flows

reflections in PDTS systems. The gas phase governing equations are numerically solved using a high-resolution shock capturing numerical method. The analysis shows that transient expansion-compression waves are formed upon external gas expansion and persist for a long time (on the time scale of a PDTS cycle) with wide fluctuations in the gas properties. The results also show that the reflected shock wave from the substrate dies out extremely fast such that micron-sized particles used in PDTS do not encounter these transients. This is due to the large lag time between the motion of a particle and the detonation wave where the upper bound of the velocity a solid particle can attain is the local gas velocity u, while the detonation front travels at a speed of $D = u + a$. The external shock wave decay was also analyzed for different reactive mixtures and flow geometries. The results show that most of the shock decay occurs within a distance of 2-3 tube diameters, and regardless of the initial shock strength, the shock decay is very fast; after about six tube diameters shocks with a wide range of initial strengths all decay to almost the same value. The results also show that the larger the tube diameter, the longer the distance the shock will travel before it decays to a certain value. This is consistent with the fact that larger diameters imply more energy, which needs longer distances to be dissipated.

The results of the shock decay problem can be related to the truncation of the computational domain and the implementation of numerical boundary conditions, where such boundary treatment should be performed at locations where the shock front has decayed sufficiently such that the gas phase evolution within the domain is not influenced by the numerical boundary conditions at the open end boundaries.

References

1. C. Li, K. Kailasanath, and G. Patnaik: "A Numerical Study of Flow Field Evolution in a Pulsed Detonation Engine," presented at *38th AIAA Aerospace Sciences Meeting and Exhibit*, Reno NV, 2000.
2. K. Ramadan and P.B. Butler: "A Two-Dimensional Axisymmetric Flow Model for the Analysis of Pulsed Detonation Thermal Spraying," accepted for publication in *Combustion Science and Technology*, 2003, *175*(9), pp. 1649-77.
3. K. Ramadan: "A Computational Study of Pulsed Detonation Thermal Spraying," Ph.D. Thesis, The University of Iowa, Iowa City, IA, 2002.
4. R.G. Schmitt, P.B. Butler, and N. French, Chemkin Real Gas: A Fortran Package for the Analysis of Thermodynamics and Chemical Kinetics in High Pressure Systems, UIME-PBB 93-006, University of Iowa, Iowa City, IA, December, 1993.
5. M.W. Chase: *NIST-JANAF Thermochemical Tables,* 4th ed., Parts 1 & 2, National Institute of Standards and Technology, Gaithersburg, MD, 1998.
6. K. Ramadan and P.B. Butler: "Analysis of Particle Dynamics and Heat Transfer in Detonation Thermal Spraying Systems," 2004, *13*(2).
7. M.J. Zucrow and J.D. Hoffman: *Gas Dynamics*, Vol. 1, John Wiley and Sons, New York, 1976.
8. Anon.: *Engineering Design Handbook, Principles of Explosive Behavior,* AMCP 706-180, U.S. Army Publication, Washington, DC, April 1972.